
Article:
Ahmed, B., Arjmandi-Tash, O., Litster, J.D. et al. (1 more author) (2023) Mechanistic modelling of spherical agglomeration processes. Powder Technology, 417. 118254. ISSN 0032-5910

https://doi.org/10.1016/j.powtec.2023.118254

---

*Corresponding author: Rachel M. Smith, Email: rachel.smith@sheffield.ac.uk Tel: +44 (0)114 2228255

Mechanistic Modelling of Spherical Agglomeration Processes

Bilal Ahmed[1], Omid Arjmandi-Tash[2], James D. Litster[1], and Rachel M. Smith[1]*

[1]EPSRC Future Continuous Manufacturing and Advanced Crystallisation Research Hub (CMAC), Department of Chemical and Biological Engineering, University of Sheffield, UK
[2]Simcyp Division, Certara, Sheffield, UK

Graphical Abstract

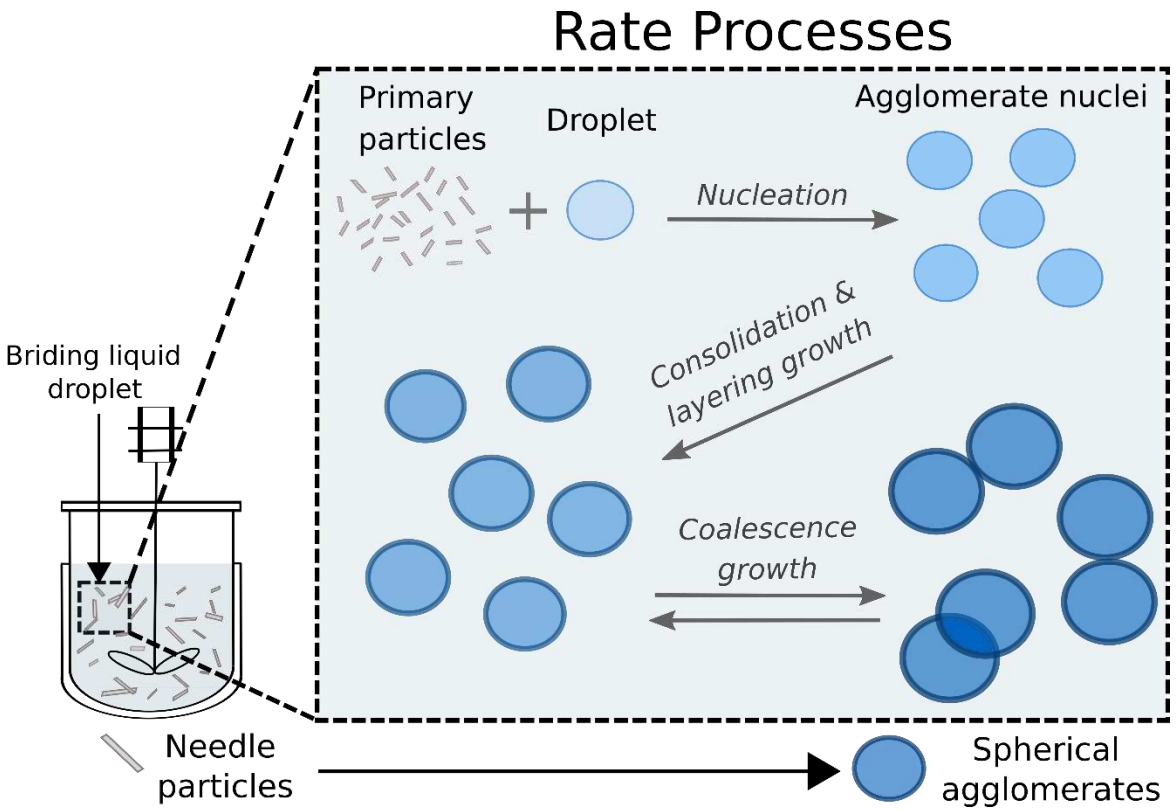

Highlights

- Population balance model predicts spherical agglomeration behaviour
- Key rate process analysed for an immersion-driven mechanism
- Bridging liquid droplet size and bridging liquid to solid ratio parameters influence both agglomerate kinetics and attributes
- Primary particle size and mixing intensity only influence agglomeration kinetics

Abstract

Spherical agglomeration is emerging as an important unit process for pharmaceutical manufacturing. However, at present, quantitative process design to control agglomerate attributes is impossible. A new population balance model to predict agglomerate attributes is presented where for the first time, all of the key rate processes that control agglomerate properties are included. A parameter sensitivity analysis is undertaken to study the effect of process parameters on agglomerate attributes. Bridging liquid droplet size and bridging liquid to solids ratio (BSR) are critical controlling parameters. Good quality agglomerates are formed over a relatively narrow range of BSR. Within this range, bridging liquid droplet size can be used to tune agglomerate size. Primary crystal size and process mixing intensity have only a modest effect on equilibrium agglomerate attributes but do impact agglomerate formation kinetics. This new model provides the basis for improved process understanding and quantitative process design of spherical agglomeration.

Keywords: spherical agglomeration, population balance model, mechanistic understanding, agglomerate size and size distribution, average liquid volume fraction

1. Introduction

The manufacturing of active pharmaceutical ingredients (API) with suitable characteristics for oral solid dosage applications requires tightly controlled particulate properties from robust unit operations. In the pharmaceutical sector, traditional batch manufacturing approaches have been the established practice. However, recent advances in continuous manufacturing have demonstrated numerous advantages for producing enhanced product properties. These range from ease of scale-up [1] to reduced variability, processing times and costs [2-4]. To enable the adoption and transition into fully integrated continuous unit operations, controlling API bulk powder properties (size, shape, surface, flow *etc.*,) with the required specifications is essential and challenging [5]. For example, insufficient control during drug substance manufacturing can lead to multiple issues with the bulk powder from poor flow, inconsistent feeding, variable die-filling, and punch sticking which ultimately produces unacceptable final tablet quality attributes [6].

Situated at the interface between drug substance and drug product manufacturing, spherical agglomeration is an emerging particle engineering technique for challenging APIs. The application of spherical agglomeration has already been investigated within industries such as natural resources including coal [7], graphite [8] and sand [9] for agglomerating a variety of products. It has also been used to agglomerate several pharmaceutical drug compounds which exhibit poor characteristics such as needle-like shapes when reliant on crystallization only [10-12] as well as poor solubility and dissolution characteristics [13]. Across the numerous studies, a key benefit to implementing spherical agglomeration is the ability to form dense and enlarged spherical particles with high bulk densities and better flow properties. Furthermore, spherical agglomerates which encapsulate and consolidate the crystal product during formation, can be subjected to direct compression which offers the fastest and simplest route to generate pharmaceutical dosage units. Currently there are four common spherical agglomeration methods; (1) Spherical Agglomeration, (2) Quasi-Emulsion Solvent Diffusion, (3) Ammonium Diffusion and (4) Crystal Co-Agglomeration. The spherical agglomeration (1) method is the most favourable approach which is performed either through the simultaneous crystal precipitation and agglomeration in suspension (post-crystallization) in the same unit operation or

through agglomeration in isolation (separate to the crystallization) which is only concerned with the agglomeration mechanisms [14]. To agglomerate directly generated or a pre-suspension of crystals, controlled addition of an immiscible or partially miscible solvent termed as the binder or bridging liquid is required and is a critical step. Importantly, the bridging liquid should possess a high affinity for the crystals in suspension to enable sufficient wetting and subsequent formation of agglomerates.

Whilst numerous studies have reported on experimental methods for the preparation of spherical agglomerates, there remains a lack of mechanistic understanding concerning the fundamental rate processes and controlling parameters. Many of the mechanisms are understood to occur through stages that are in parallel with wet granulation: (i) wetting and nucleation of the particles by the bridging liquid; (ii) consolidation and growth of agglomerate nuclei and; (iii) breakage and attrition [15, 16]. The wetting of crystals by the bridging liquid droplets and the relative size ratio between the two entities can direct the formation of agglomerate nuclei through two separate mechanisms (distribution & immersion). If the bridging liquid droplets are smaller than the suspended crystals (primary particles), a distribution mechanism will occur. Here, the crystals become 'coated' by droplets over time which allows them to aggregate to form an initial agglomerate nucleus. On the other hand, if the bridging liquid droplets are larger than the suspended crystals, an immersion mechanism occurs. Crystals will penetrate inside the droplets over time and form an initial agglomerate nucleus. The immersion mechanism is preferred as the final agglomerates display more uniform particle size distributions (PSD), higher sphericity, and density [17]. The occurrence and interplay of these mechanisms can be found from several reported studies [18-20].

Recently, two new agglomerate nucleation models were introduced to predict and describe the wetting and nucleation kinetics during an immersion mechanism [21]. A dimensionless number termed the *agglomerate nucleation number* was developed to predict the kinetics of agglomerate nucleation by layering. The kinetics were identified on the basis of three regimes: *immersion rate limited*; *collision rate limited* and; *intermediate regime* which describes the system to be limited by both the immersion

and collision rate. The *immersion rate limited regime* assumes a packed layer of stationary particles is always available on the surface of the bridging liquid droplets where subsequent immersion is limited by the wetting (capillary) action of these particles. In this case, the agglomerate size increases with the square root of time. For the *collision rate limited regime*, immediate wetting and suction of particles inside the bridging liquid droplet occur; however, the process is limited by the arrival of particles to the surface of bridging liquid droplets. The agglomerate size, therefore, increases linearly with time. Both models also assume the agglomerate nucleus grows by the formation of a shell of a constant liquid volume fraction.

For consolidation and growth of agglomerates, certain studies have developed agglomerate rate kernels to account for several particle-particle interactions: *agglomerate-agglomerate collisions*; *crystal-crystal collisions,* and; *coalescence of agglomerate nuclei* with a focus on the formation of liquid bridges between the agglomerate nuclei or between crystal particles [17, 22-24]. One particular study developed a coalescence rate kernel on the basis of a *meeting probability* term and *coalescence efficiency* term for agglomerates in contact [25]. The *meeting probability* is defined as the function of the target efficiency, agglomerate sizes and collision velocity. As for the *coalescence efficiency* term, the model is a function of adhesion and separation forces that act on the two deformed agglomerates upon their impact. Overall, the model system displayed good agreement with experimental data (PSD & porosity) which was validated for salicylic acid in an aqueous solution and chloroform as the chosen bridging liquid.

Considering the approaches taken in literature to understand and describe a spherical agglomeration process, a comprehensive model which incorporates all of the identified key mechanistic rate phenomena is lacking. Population balance modelling is an attractive tool for simulating agglomerate evolution over time and was previously demonstrated for an antisolvent crystallization system of benzoic acid with agglomeration [26]. However, to our knowledge there is no study to date which includes the critical stages of wetting and nucleation as well as agglomeration through a mechanistic-driven population balance model for an agglomeration in suspension method.

In this work, a novel population balance model framework is developed and investigated for mechanistic understanding and prediction of product properties for a spherical agglomeration process. We specifically study the agglomeration in suspension technique driven by the immersion mechanism and incorporate customized layering and coalescence rate kernels for analysis of the concomitant rate phenomena. This includes, wetting of the primary particles by the bridging liquid droplets and subsequent agglomerate nuclei formation, consolidation and growth of agglomerates due to layering and growth of agglomerates by coalescence (Figure 1). Firstly, we outline the methodology used to integrate the mechanistically relevant rate equations into the population balance model framework to characterize the aforementioned stages. We then examine the influence of important formulation and process parameters which consists of the starting primary particles size, bridging liquid droplet size, true bridging liquid to solids ratio, and agitation rate on the agglomerate size and size distribution and average liquid volume fraction over time.

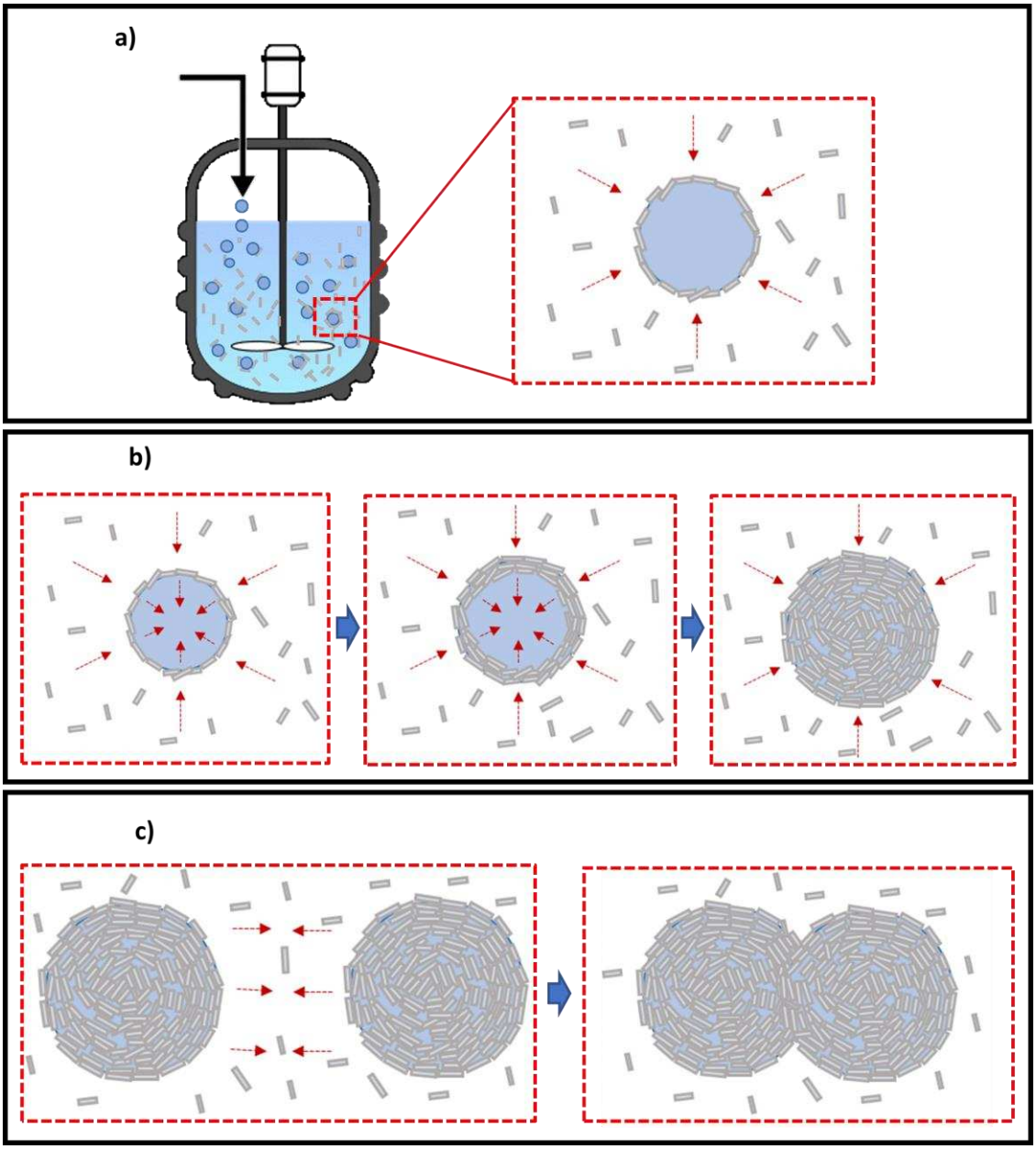

Figure 1. Schematic of the rate processes included within the population balance model: (a) bridging liquid addition and agglomerate nucleation; (b) consolidation and growth of agglomerates by layering; (c) growth of agglomerates by coalescence.

2. Mathematical Modelling

The governing 1-D population balance equation to simulate the evolution of agglomerates attributes over time is given by:

$$\frac{\partial V n_a(x,t)}{\partial t} + \frac{\partial V[G(x,t)n_a(x,t)]}{\partial x} = \dot{Q}_{in} n_{a,in}(x,t) - \dot{Q}_{ex} n_{a,ex}(x,t) + V\left[\dot{b}_{a,nuc}(x,t) + \dot{b}_{a,aggl}(x,t) - \dot{d}_{a,aggl}(x,t)\right] \quad (1)$$

where, $n_a(x,t)$ is the number density (no/m^4) representing the agglomerates of diameter x at time t. V is the suspension volume (m^3). $G(x,t)$ is the growth rate of agglomerates (m/s) by layering. $\dot{Q}_{in}$ and $\dot{Q}_{ex}$ are the volumetric flows (m^3/s) entering and leaving the system, and $n_{a,in}(x,t)$ and $n_{a,ex}(x,t)$ are the inlet and exit size distributions (no/m^4). $\dot{b}_{a,nuc}(x,t)$ is the agglomerate nucleation rate (no/(m^4.s)) due to bridging liquid addition into the suspension and wetting of crystals by the bridging liquid droplets. $\dot{b}_{a,aggl}(x,t)$ and $\dot{d}_{a,aggl}(x,t)$ are birth and death rates of agglomerates due to coalescence (no/(m^4.s)). Breakage and attrition of the agglomerates is not considered due to a limited number of reported studies on the mechanisms involved [15].

gPROMS FormulatedProducts v2.2 (Siemens, Process Systems Enterprise, Ltd.) was used as the platform to develop and solve the population balance equation for spherical agglomeration. It is known that many of the mechanisms in a spherical agglomeration process are analogous to a high shear wet granulation process and therefore, the model flowsheet configured in gPROMS FormulatedProducts is adapted from the high wet shear granulation unit. Customized mechanistic rate kernels were then built within the model library which are selected and incorporated within the population balance framework. The rate processes and parameters of the model are described in the following sections.

2.1. Bridging Liquid Addition and Agglomerate Nucleation

After the addition of bridging liquid droplets into the system, the formation of agglomerate nuclei is assumed to occur based on the model of Barrasso and Ramachandran [27]:

$$\dot{b}_{a,nuc}(x,t) = \frac{\dot{L}_{in,p} n_d(x,t)}{V_d} \tag{2}$$

Upon the addition of bridging liquid droplets with total a volumetric flow rate of $\dot{L}_{in}$ (m^3/s) and number density of $n_d(x,t)$ (no/m^4) into the vessel, they either wet the fine crystals and form new agglomerate nuclei or they attach to the existing agglomerates and increase their liquid content. The fraction of liquid added to the fine crystals and forming new agglomerate nuclei ($\dot{L}_{in,p}/\dot{L}_{in}$), is assumed to be equal to the ratio of the volume of the crystal to the total volume of particles (crystals+ agglomerates) in the system. Here we also assume that the recently generated agglomerate nuclei have the same size, D_d, and volume, V_d, as their constitutive bridging liquid droplets and the initial liquid volume fraction of the agglomerate nuclei is one. This assumption will allow us to differentiate the kinetics of bridging liquid addition and agglomerate nucleation from the kinetics of consolidation and growth of agglomerates due to wetting of crystals by bridging liquid droplets and subsequent immersion of crystals inside the droplets.

2.2. Consolidation and Growth of Agglomerates by Layering

The consolidation and growth rate of agglomerates in the suspension depend on the wetting kinetics of crystals by bridging liquid droplets and subsequent immersion of crystals inside the droplets (i.e. in an immersion mechanism in which the bridging liquid droplets are larger than the particles to be agglomerated). In a recent publication [21], we developed two new mathematical models for the kinetics of wetting of crystals and their immersion inside the bridging liquid droplets: *immersion rate limited regime* and *collision rate limited regime* where full derivation of the equations describing these phenomena can be found. We will use these models to predict the kinetics of consolidation and growth of agglomerate nuclei in the population balance framework where we define the growth rate of an individual agglomerate as:

$$G(x,t) = \left(\frac{\partial x}{\partial t}\right)_x \tag{3}$$

According to Arjmandi-Tash et al. [21], the time evolution of agglomerate size in an agglomeration in suspension process is given by:

$$\left(\frac{\partial x}{\partial t}\right) = C_{growth}\frac{2\Psi D_p \gamma cos\,\theta}{15\mu_d x}(1-\varphi_{cp})\varphi_{cp} \tag{4}$$

for an *immersion rate limited regime* or

$$\left(\frac{\partial x}{\partial t}\right) = C_{growth}2\alpha\left[u(D_p)^2 + u(D_d)^2\right]^{\frac{1}{2}}\varphi_{P_b}(t) \tag{5}$$

for a *collision rate limited regime*.

In Eqs. (4)-(5), D_p and Ψ are diameter and sphericity factor of crystal particles, respectively; γ is interfacial tension between bridging liquid and mother solution; θ is bridging liquid/solid contact angle at three-phase bridging liquid/mother solution/solid contact line; μ_d is the viscosity of the bridging liquid; $\varphi_{cp}$is critical-packing liquid volume fraction; α is target efficiency; $u(D_p)$ and $u(D_d)$ are the particle-mother solution and bridging liquid droplet-mother solution relative velocities, respectively; C_{growth} is a kinetic parameter to be determined by the agglomeration experiments; φ_{Pb} defines the crystal volume fraction in the bulk mother solution. φ_{Pb} remains constant in a continuous, well-mixed system at steady state (mixed-suspension, mixed-product removal, MSMPR) whereas, in a batch agglomeration system, it decreases due to immersion inside the bridging liquid droplets. The population balance in conjunction with a mass balance for the system in gPROMS FormulatedProducts enables us to account for any changes in the crystal volume fraction in the bulk mother solution during the agglomeration process.

The agglomerate nucleation number, $AgNu$, predicts different regimes of agglomeration; *immersion rate limited* and *collision rate limited* and it determines which of the above correlations should be used to predict the growth rate of agglomerates in the population balance framework. For a system with an agglomerate nucleation number, *AgNu*, larger than one, the process of agglomerate nucleation is limited by the immersion rate. Thus, the growth rate can be found by

Eq. (4). On the other hand, if the agglomerate nucleation number, *AgNu*, is lower than one, the process is controlled by the collision and arrival of the particles at the bridging liquid droplet surfaces. The growth of agglomerates can be obtained by Eq. (5).

2.3. Growth of Agglomerates by Coalescence

The growth of larger agglomerates can also occur due to the possible coalescence during agglomerate-agglomerate impact. To account for this growth, a mechanistic coalescence kernel was implemented on the basis of Blandin *et al*. model [25], which is expressed as the product of the meeting probability and the coalescence efficiency. The main equations used for the birth and death rates of agglomerates due to coalescence in our population balance framework are listed:

$$\dot{b}_{a,aggl}(v,t) = \frac{1}{2}\int_0^v K(v', v-v', t)(n(v', t)n(v-v', t)dv' \tag{6}$$

$$\dot{d}_{a,aggl}(v,t) = \int_0^\infty K(v, v', t)n(v,t)n(v', t)dv' \tag{7}$$

Where K is the coalescence kernel and v, v' represent the agglomerate volume. The coalescence kernel is defined as:

$$K(v, v', t) = K(i, j, t) = f(i, j, t)eff(i, j, t) \tag{8}$$

$f(i, j, t)$ determines the meeting probability of agglomerates and $eff(i, j, t)$ is the coalescence efficiency term. The meeting probability considers the encounter of agglomerates and is a function of the hydrodynamics of the system:

$$f(i, j, t) = \alpha(i, j, t)\frac{\pi}{4}(x_i + x_j)^2\left[u(x_i)^2 + u(x_j)^2\right]^{1/2} \tag{9}$$

Here, $\alpha(i, j, t)$ is the target efficiency, x is the characteristic sizes of the agglomerates and u (x) is the agglomerate-mother solution relative velocity which is calculated from the mean square of the particle-liquid relative velocity. The coalescence efficiency

term was introduced to correct for the meeting probability and to calculate the maximum size that agglomerates eventually reach:

If $f_{adh}(i,j,t) \geq f_{sep}(i,j,t)$:

$$eff(i,j,t) = \frac{f_{adh}(i,j,t)}{f_{sep}(i,j,t)} - 1 = C_{eff} \frac{\left[\frac{def^{max}(i,j,t)}{\frac{D_p}{2}}\right]^2 \left(1-\varphi(t)\right) F_{bridge} \frac{x_i^2 + x_j^2}{x_i^3 + x_j^3}}{\rho_L [\varepsilon(x_i + x_j)]^{\frac{2}{3}} x_i^2} - 1 \quad (10)$$

If $f_{adh}(i,j,t) < f_{sep}(i,j,t)$: $eff(i,j,t) = 0$ (11)

$f_{adh}(i,j,t)$ is the adhesive force, $f_{sep}(i,j,t)$ is the shear-induced disruptive force, F_{bridge} is the bridging liquid bridge force between the two crystal particles, $def^{max}(i,j,t)$ is the radius of the contact surface, D_p is the mean size of the crystal particles, ρ_L the density of the mother solution, C_{eff} the coalescence efficiency coefficient, ε is the average energy dissipation. Expressions corresponding to the terms, $\alpha(i,j,t)$, $u(x)$, $f_{adh}(i,j,t)$, $f_{sep}(i,j,t)$, F_{bridge} and $def^{max}(i,j,t)$ can be found in detail [25]. The average energy dissipation, ε, was estimated using a power number correlation as a function of suspension volume, V, agitation rate, n_r, and impeller diameter, d_{imp}.

3. Model Parametrisation

3.1. Process Scheme

The population balance model was set up and solved using the gPROMS process simulation platform. A sketch of the model process is shown in Figure 2 to depict a typical agglomeration in suspension technique.

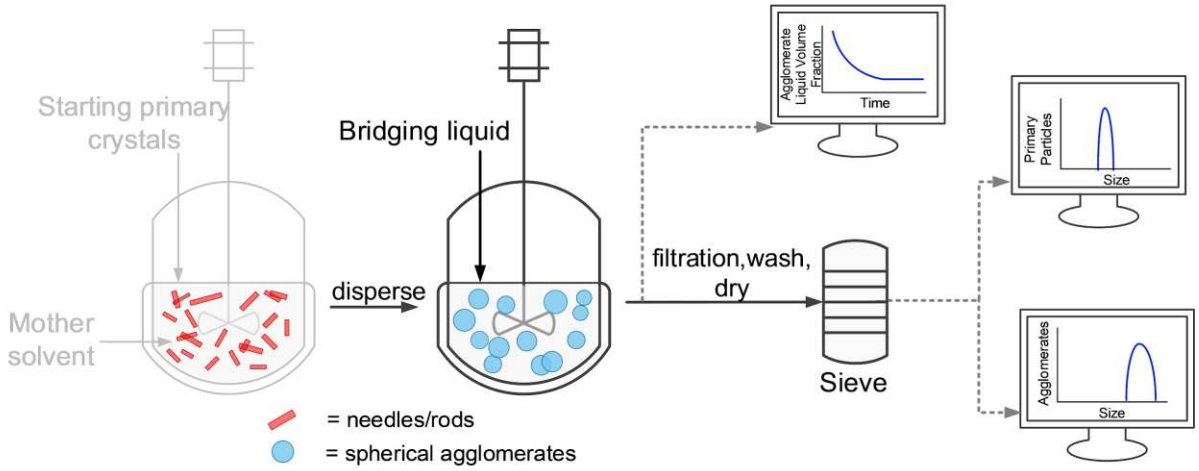

318

319 **Figure 2.** Sketch of process flowsheet used to simulate the spherical agglomeration
320 process (batch), mechanisms and the product attributes.

321

322 Before the addition of a bridging liquid, an assumed insoluble suspension of crystals
323 is typically dispersed and held at equilibrium for some time. Incorporating the key
324 constitutive rate equations as described in Section 2, the behaviour and performance
325 of the model is then analysed upon immediate addition of the bridging liquid droplets.
326 Whilst the governing 1-D population balance equation (Eqn. 1) presents the
327 opportunity to model both a batch or continuous process, in this study a batch process
328 was selected.

329

330 Product properties such as the particle size distributions are analysed and determined
331 using a dry sieving unit consisting of 101 incremented sieves (non-linearly) with an
332 aperture range from 0.01 to 3500 μm. The choice of the incremented sizes and
333 aperture range were based on input measured data of the crystal particles. A
334 logarithmic particle size distribution is then generated and reported as a volume %.
335 The average liquid volume fraction inside the whole volume of the growing
336 agglomerate nucleus was also examined over time from the following expression:

337

$$\varphi_{avg}(t) = \frac{\left({}^{D_d}/_{2}\right)}{H_2(t)} \tag{12}$$

338

339 Where the size of the agglomerate nucleus, $H_2(t)$ can be found by:

$$H_2(t) = \frac{D_d}{2} + \left(\frac{\Psi D_p \gamma \cos\theta}{15\mu_d}\left(1 - \varphi_{cp}\right)\varphi_{cp} t\right)^{1/2} \quad (13)$$

For an *immersion rate limited regime* or:

$$H_2(t) = \frac{D_d}{2} + \frac{D_d}{2TBSR}\left(1 - \exp\left(\frac{2\alpha\left[u\left(D_p\right)^2 + u(D_d)^2\right]^{1/2}\varphi_{P_{b0}} TBSR}{D_d} t\right)\right) \quad (14)$$

For a *collision rate limited regime*.

Therefore, at the start of the agglomeration process, φ_{avg} = 1 at t = 0 (bridging liquid only). The average liquid volume fraction was incorporated within the layering kernel in the gPROMS software which considers the density and inter-particle voidage. Considering the model assumptions, the unit operation is a well-mixed system and the dissolution of fine powder and agglomerate phases is negligible. The temperature of the process is constant and uniform at 25 ºC. The bridging liquid droplet sizes have consistent uniformity at the specified mean size with a fixed standard deviation (20 μm) and is immiscible with the mother solution. Bridging liquid to solids ratio (BSR) is therefore the same as the true bridging liquid to solids ratio (TBSR).

3.2. Selection of Model Parameters and Operating Conditions

A sensitivity analysis of selected model parameters and operating conditions (Table 1 & Table 2) was investigated. Whilst numerous model parameters are included within the population balance model framework (Eqn. 1), studying the impact of each parameter would be unfeasible. Therefore, the selected parameters and chosen ranges are based upon reported literature values, several published experimental studies and reasonable estimations. The focus of this work was to study the bulk formation and behaviour of agglomerates and thus, high values were chosen for kinetic growth parameters. Additional parameters appearing in the different rate kernels, were based on already measured values for the agglomerating system,

Lovastatin in water as the mother solution and methyl isobutyl ketone (MIBK) as the bridging liquid which was studied as the system of interest [21, 28]. Lovastatin is an anti-cholesteremic BCS (Biopharmaceutical Classification System) class II drug used in the treatment for hypertension and displays poor solubility and dissolution properties. The API encompasses a complex chemical structure and is typically crystallised in a needle-like form making it desirable for a spherical agglomeration process.

Table 1. Selection of formulation and material properties used in the simulations.

Stage	Parameter	Set point
All	Mother solution viscosity, μ_L (Pa.s)	8.9×10^{-4}
	Mother solution density, ρ_L (kg/m^3)	1000
	Bridging liquid-mother solution interfacial tension, γ (N/m)	1.01×10^{-2}
	Bridging liquid viscosity, μ_d (Pa.s)	5.8×10^{-4}
	Bridging liquid density, ρ_d (kg/m^3)	802
	Crystal skeletal density, ρ_p (kg/m^3)	1100
	Particle-bridging liquid contact angle in solvent, θ_2 (º)	30
Consolidation & Layering	Sphericity factor for crystal particles, Ψ (-)	0.43
	Critical packing liquid volume fraction, φ_{cp} (-)	0.36
	C_Growth, (-)	0.69
Coalescence	Meeting probability, $f(i,j,t)$ (-)	1
	Coalescence efficiency, $eff(i,j,t)$ (-)	0.3×10^{-4}
	Separation distance, α (m)	0.1×10^{-5}
	Half-filling angle, β (º)	70
	BSR min, (m^3/m^3)	0.01
	BSR max, (m^3/m^3)	0.7

Table 2. Selection of operating conditions and ranges used in the simulations.

Process Parameters	Set point
Simulation duration (min)	22
Crystal loading, C_s (wt.%)	5
Temperature, (ºC)	25
Suspension volume, $V_{suspension}$ (mL)	500
Impeller diameter, d_{imp} (m)	0.035
Bridging liquid addition rate, Q_d (g/min)	3
Mean initial particle size, D_p (μm)	40-120
Agitation rate, (RPM)	200-600
Bridging liquid addition time, t (min)	1-6
Bridging liquid droplet size, D_d (μm)	100-400

3.3. Solution of the Population Balance Equation

All simulations were run in gPROMS v2.2 (Siemens, Process Systems Enterprise Ltd.) The standard gPROMS solver for differential-algebraic equations is DAEBDF which was used as the numerical method to solve the population balance equations. A high resolution finite volume scheme with flux limiting function (HRFVS-FL) was used which includes the discrete rate processes (nucleation & coalescence) and was evaluated at the particle size midpoints whereas the continuous rate processes (consolidation & layering) are evaluated at the boundary conditions to determine the kinetics of growth. The size domain has been divided for the discretization of the population balance equation according to a geometrical grid (non-linear), giving smaller step sizes to contribute to a higher numerical accuracy of the solution and, improving the PSD resolution at initial times. A logarithmic grid was chosen with 64 bins for the agglomerate size distribution (1 – 3500 μm).

4. Results & Discussion

4.1. Reference Conditions

Prior to analysis of the selected formulation and process parameters within the specified ranges, an example trend is shown (Figure 3) to demarcate the key features and mechanisms during spherical agglomeration by the immersion mechanism.

Figure 3 displays the evolving average agglomerate liquid volume fraction, φ_{avg} (-) and median particle size, D_{50} (μm) for the total particle population over time (a) as well as the fraction of non-agglomerated and agglomerated particles (b). The simulated process trends are analysed upon immediate addition of the bridging liquid at 0 min with a flow rate of 3 g/min. After 3.35 min, the bridging liquid addition is stopped and the simulation continues for 22 min. In this analysis (Figure 3), the region between 0 to 10 min is closely examined as there is a minimal change from the predicted trends during 10 to 22 min.

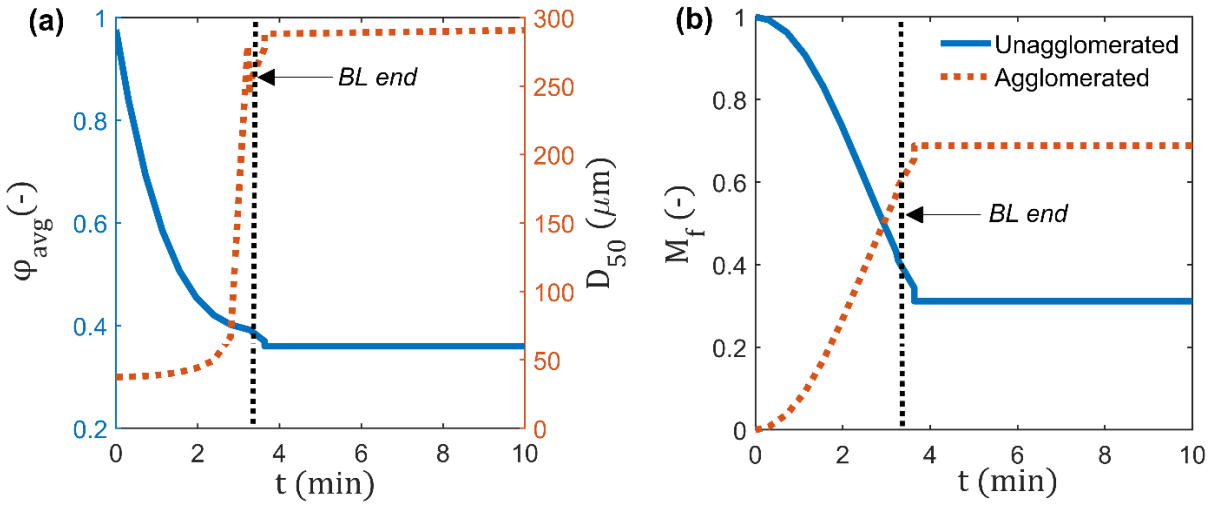

Figure 3. Simulated profiles showing the (a) average agglomerate liquid volume fraction, φ_{avg} and median particle size, D_{50} over time; (b) the mass fraction, M_f for non-agglomerated and agglomerated particles over time. Key parameter values prediction were: bridging liquid (BL) droplet size, D_d = 200 μm; BL addition rate, Q_d = 3 g/min, BL addition time, t = 2 min (BSR = 0.55); agitation rate = 400 RPM (ε = 0.0023) and; mean initial primary particle size, D_p = 40 μm. A simulation time of 22 min was selected for all conditions.

During the bridging liquid addition stage (0 to 3.35 min) with a fixed droplet size (D_d = 200 μm) to the pre-suspended crystals (D_p = 40 μm) resulted in a rapid decline of the φ_{avg} (1 to 0.39). A slow increase during initial wetting followed by a sharp incline in the D_{50} profile (40 to 260 μm) during growth occurred until the final addition point Figure 3, (a). Simultaneously, the fraction of unagglomerated (primary particles) in suspension was reduced (60%) compared to the fraction of agglomerated particles (Figure 3, b) which increased over time (0 to 3.35 min).

The results confirm wetting, agglomerate nucleation and growth by consolidation and layering to be prevalent during the bridging liquid addition stage. Operating in the *collision rate regime* (Eqn. 5) is predicted as the agglomeration nucleation number, $AgNu = 4.56\times10^{-6}$ is less than 1. After the final addition of the bridging liquid droplets (> 3.35 min), a minimal increase in the D_{50} and a small decrease in the φ_{avg} are observed. Further growth to form larger agglomerates by coalescence mechanisms can occur (Figure 1) however in this case, coalescence is negligible as the agglomerate properties are unchanged after 4 min (Figure 3).

Decoupling the mechanisms in a spherical agglomeration process is challenging. However, through population balance modelling one can begin to understand and provide mechanistic insight into the concurrent wetting and nucleation, consolidation and growth phenomena from the effect of selected formulation properties and process conditions on the evolution of agglomerate properties.

4.2. Effect of Formulation and Process Parameters

The following section presents a local sensitivity analysis from the selected input variables: mean initial primary particle size, D_p (μm); mean droplet size, D_d (μm); bridging liquid to solids ratio (BSR); and the agitation rate (RPM). To ensure the immersion mechanism was maintained across all conditions, D_d was kept larger than D_p. Furthermore, under the given material system with fixed input parameters (Table 1 & Table 2), $AgNu$ remained below 0.01 and as a result, the system was always within the collision rate regime.

Figure 4 and Figure 5 show the effect of the selected formulation and process variables on the average liquid volume fraction, φ_{avg}, and median agglomerate size, D_{50}. Increasing the primary particle size (40 to 160 μm) increases the initial wetting and nucleation rate because the collision rate increases with particle size. The agglomeration process is complete within 6 min for 40 μm particles but reduces to 3.50 min for 160 μm particles (Figure 4, (a-b)). On the other hand, increasing the droplet size (100 to 500 μm) prolonged the timescale for immersion of crystals within the droplets when compared to varying the initial primary particle size. This is seen from the φ_{avg} trends (Figure 4, (c)) where D_p = 100 μm produced a faster reduction in φ_{avg} than D_p = 500 μm during the full wetting period (0 to 3.35 min). Selecting a $D_p > 300$ μm lengthened the nucleation process during the wetting period and subsequent time to agglomerate completion. Increased growth rates with larger final sizes were achieved as observed from the median agglomerate size, D_{50} profiles (Figure 5, (d)).

The BSR value corresponded to different total bridging liquid addition times and so the final addition point varied from 2 to 5 min (Figure 5, (a-b)). Minimal differences in the overall φ_{avg} profiles were observed with a BSR range of 0.15 to 0.75 whereas the highest selected value of 2 had a substantial impact on φ_{avg} over time (Figure 5, (a)). This impact is also observed in the full D_{50} profile (Figure 5, (b)) indicating uncontrolled agglomeration. Operating within the BSR range from 0.15 to 0.75 increased the agglomerate median size. However, for BSR < 0.35 there is insufficient bridging liquid content available to promote agglomerate growth (Figure 5, (b)).

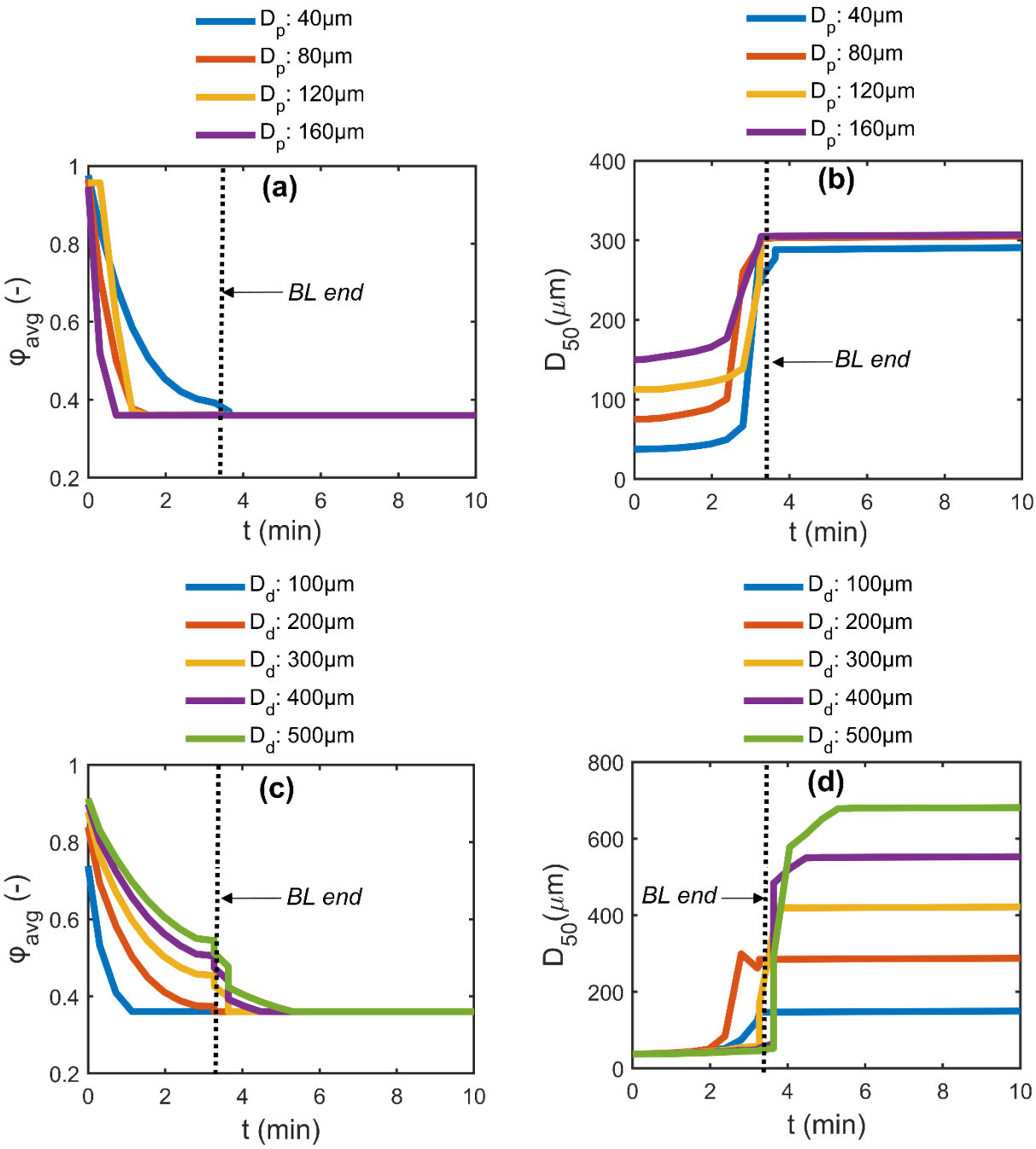

Figure 4. Sensitivity of time evolution of the average agglomerate liquid volume fraction, φ_{avg} and median particle size, D_{50} to (a-b) initial mean primary particle size, D_p (μm) and; (c-d) mean bridging liquid droplet size, D_d (μm).

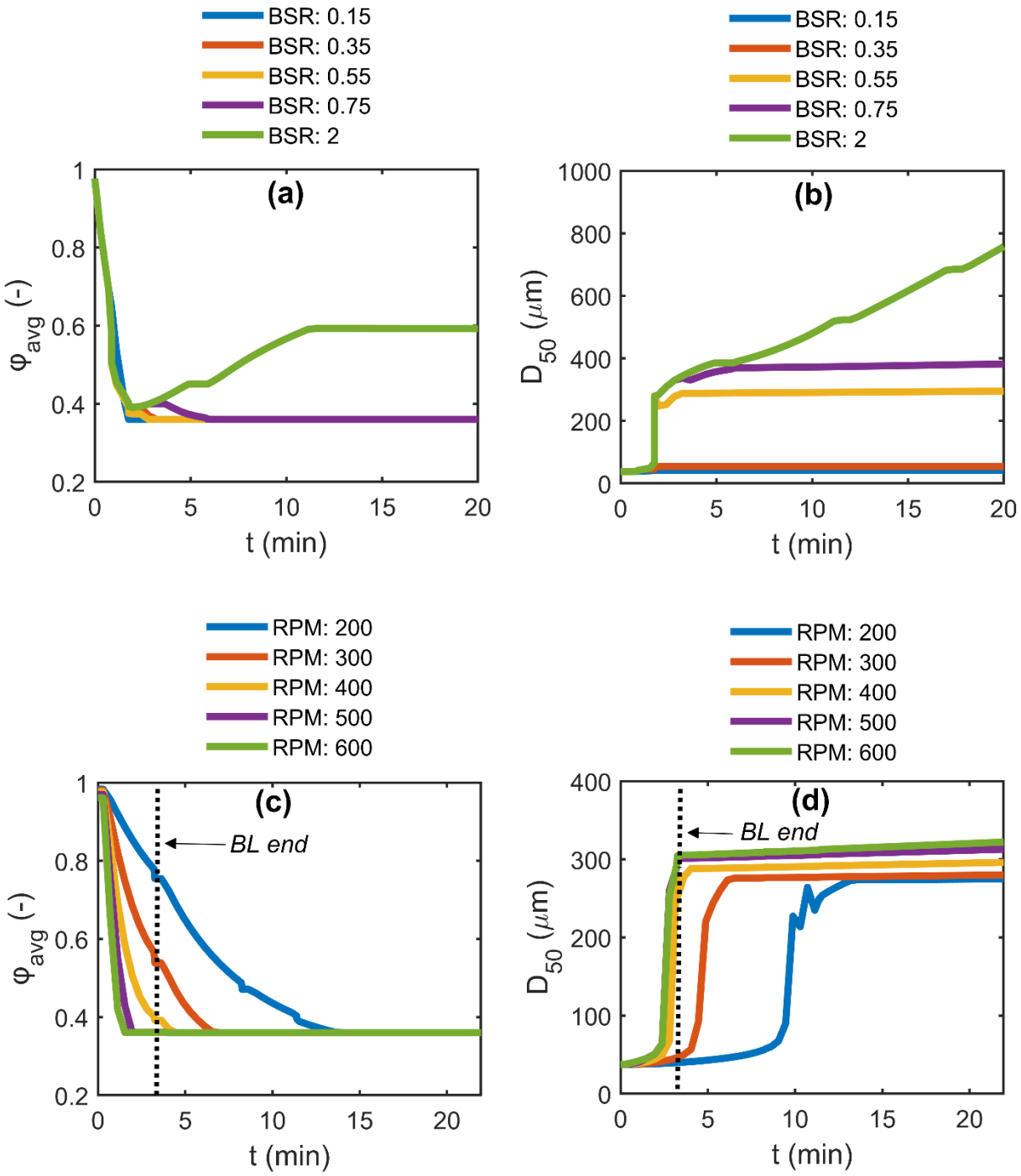

Figure 5. Sensitivity of time evolution of the average agglomerate liquid volume fraction, φ_{avg} and median particle size, D_{50} to (a-b) bridging liquid to solids ratio (BSR) and (c-d) agitation rate (RPM).

Nucleation and agglomeration kinetics were highly sensitive to the agitation rate parameter (Figure 5, (c-d)). For instance, the time to agglomerate completion at 200 RPM was 15 min whereas at 600 RPM, 3.50 min is required for agglomerate completion (Figure 5, (c-d)). This substantial difference in time to agglomerate completion is due to increased mixing intensity within the batch reactor which increases the collision frequency between droplets and crystals, therefore, accelerating the immersion process during the wetting stage.

Figure 6 and Figure 7 show how the full size distribution changes with time. Here, the size distributions show both the primary particles (smallest size mode) and the agglomerates (larger size mode). As growth by consolidation and particle layering occurs, the first mode reduces in size as primary particles are captured by droplets. The height of the second mode increases and agglomerate size also increases. In addition to the selected conditions shown in Figure 4 and Figure 5, full PSDs for all conditions are captured and displayed within the appendix.

Reduction in primary particles and growth of agglomerates from 0 to 22 min is shown for both the mean initial primary particle size, D_p and the droplet size, D_d. Tuning the droplet size had a clear impact on the final agglomerate size as shown from the PSD evolution for D_d = 500 μm and 200 μm in Figure 6, (d). A high BSR value (2) was shown to have a significant impact on the mean agglomerate size. However, at low BSR (0.15), the effect was negligible (see Figure 7 (a)-(d)). Although the primary particles have been completely removed in Figure 7 (b), agglomeration is still ongoing (see Figure 5, (b)). Agglomerate coalescence continues as a consequence of deformation and compaction mechanisms throughout the growth-period which can lead to paste formation. Similar to Figure 5 observations, varying the agitation rate had a minimal impact on the final agglomerate size distributions as opposed to the time to agglomerate completion kinetics (Figure 7, (c-d)).

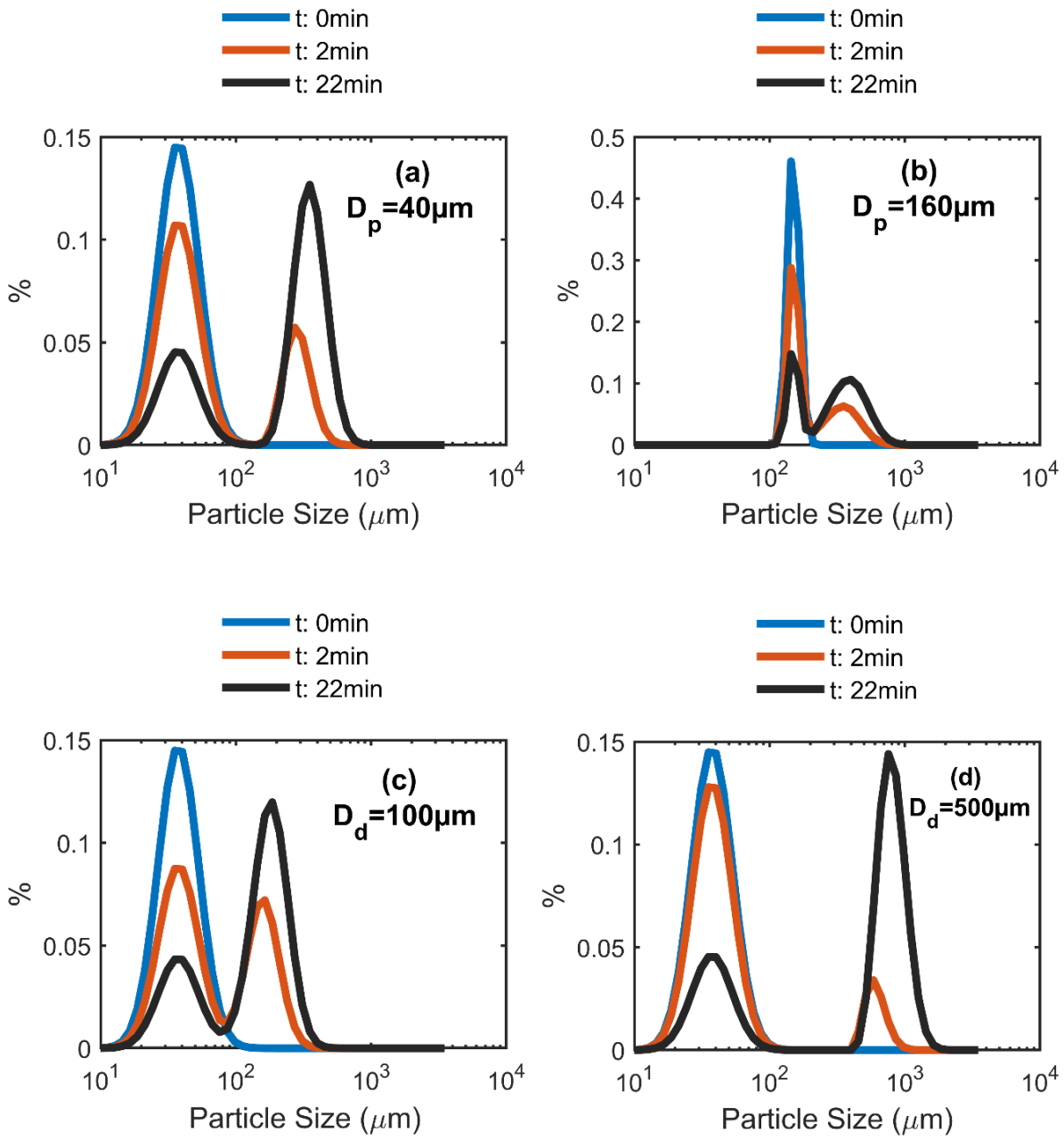

Figure 6. Evolving agglomerate size distributions over time for an initial mean primary particle size, D_p (μm) of (a) 20 μm and (b) 120 μm as well as for mean bridging liquid droplet sizes, D_d (μm) of (c) 100 μm and (d) 500 μm.

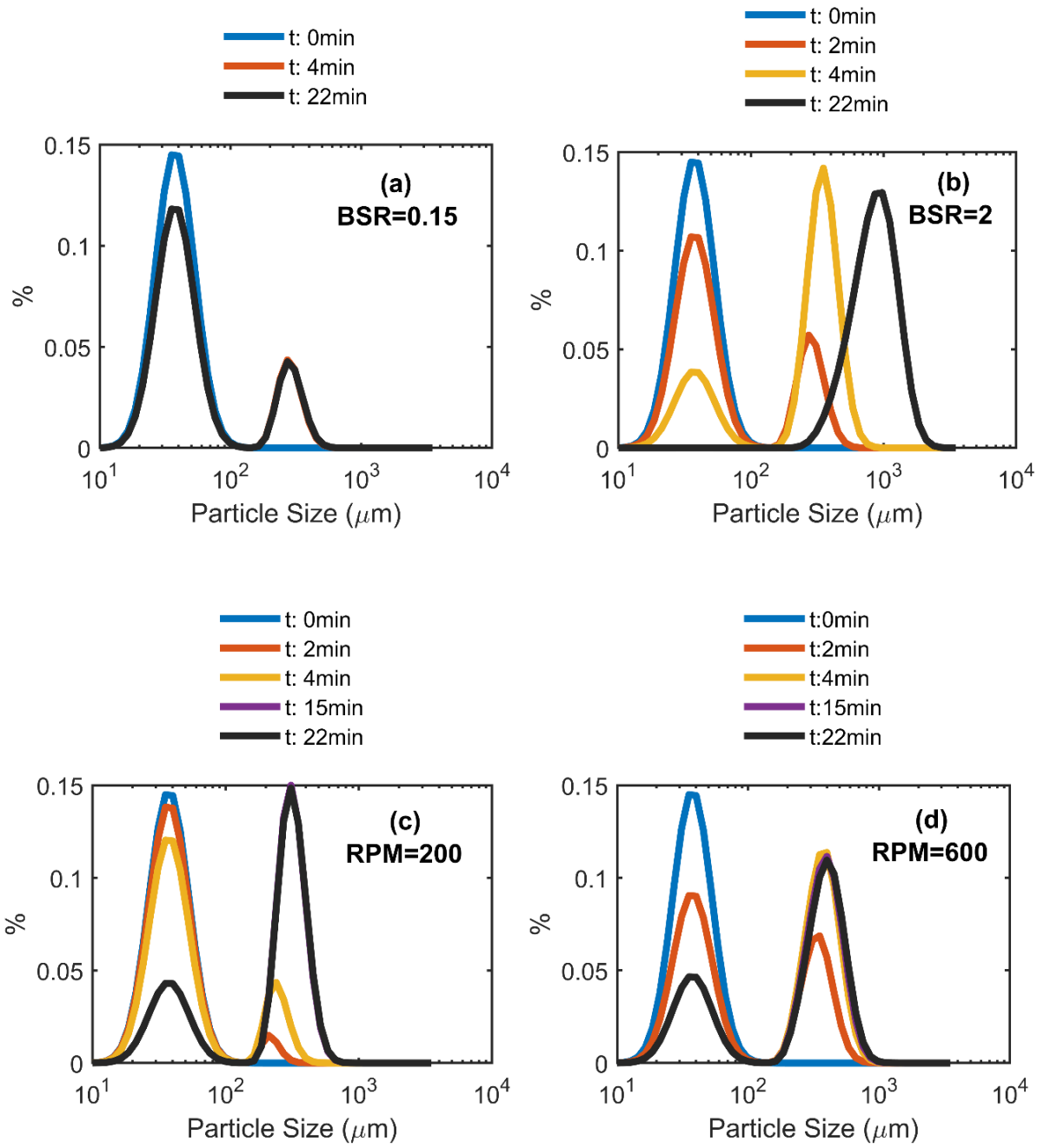

Figure 7. Evolving agglomerate size distributions over time for BSR of (a) 0.15 and (b) 2 as well as for an agitation rate, (RPM) of (c) 200 and (d) 600.

The impact of the selected parameters on various particle size statistics (D_{10}, D_{50} and D_{90}) are shown in Figure 8. Bridging liquid droplet size and BSR have the most profound effect on the final agglomerate sizes achieved. Interestingly, when comparing the trends in Figure 8, (b & c), the median and larger sizes (D_{50} & D_{90}) show an increasing trend whilst the smaller sizes represented by D_{10} remains largely unchanged for changes in D_d as opposed to the BSR parameter and within the

selected parameter ranges. In contrast, there is minimal change in the particle size distribution statistics from varying the initial mean primary particle size and agitation rate.

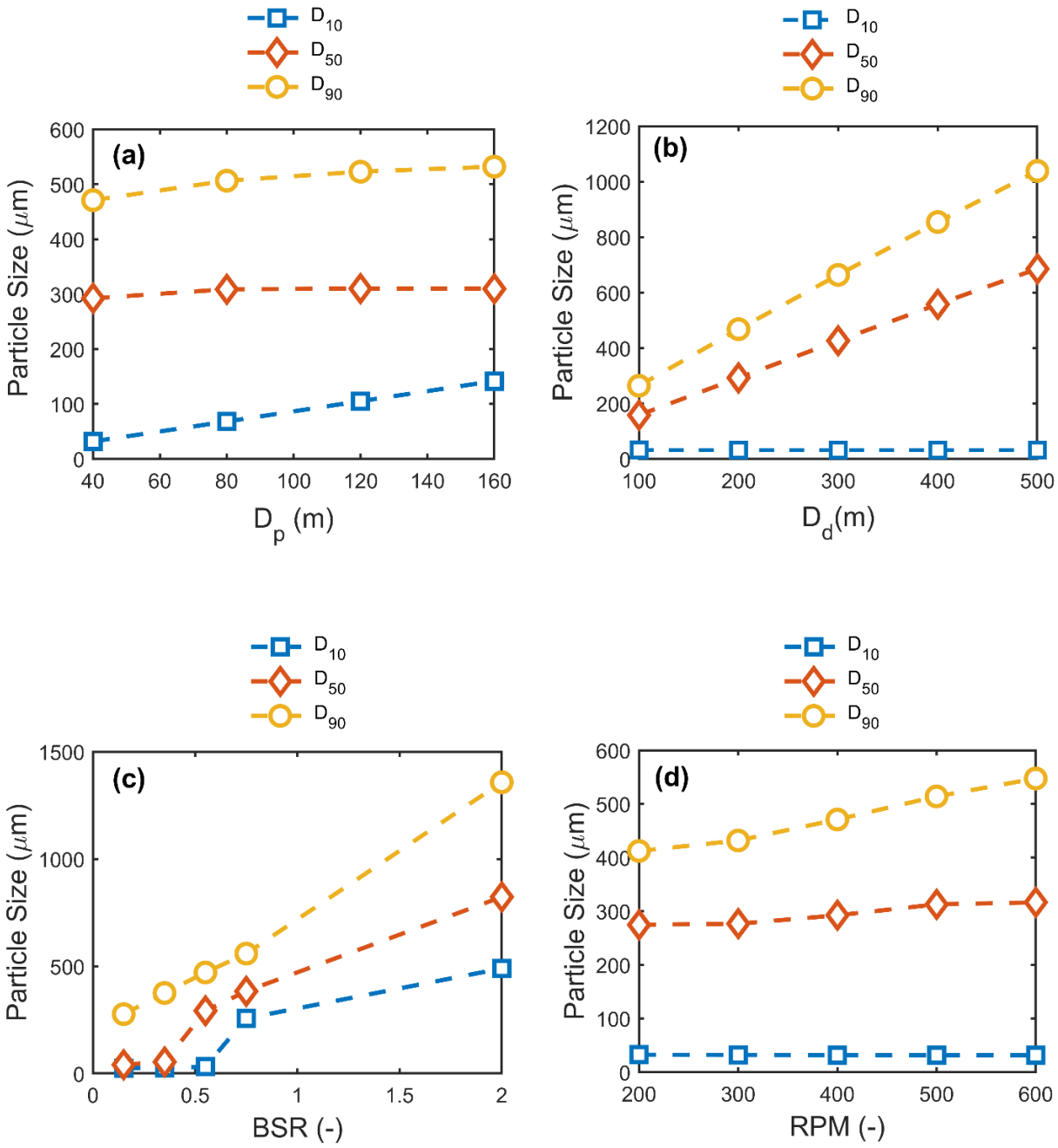

Figure 8. Final agglomerate size values (D_{10}, D_{50}, D_{90}) plotted as a function of varying the (a) initial mean primary size, D_p (μm) (b) mean bridging liquid droplet size, D_d (μm) (c) bridging liquid to solids ratio (BSR) and (d) agitation rate (RPM).

5. Conclusions

A population balance model has been developed and was used to study a spherical agglomeration process. The simulated results (agglomerate size and size distribution, average liquid volume fraction) from the selected formulation and process parameters (initial primary particle size, bridging liquid droplet size, true bridging liquid to solids ratio, and agitation rate) revealed important mechanistic insights and tuneable conditions to produce desirable agglomerates. Bridging liquid droplet size and BSR had the most influence on both the nucleation and agglomeration kinetics, time to completion, and the final equilibrium agglomerate attributes. This effect was most noticeable when tuning the size of the bridging liquid droplets which generated a range of final agglomerate size and size distributions. The model can also be used to set a safe operating range for the BSR parameter to produce stable agglomerates which in this case were from 0.35 to 0.75. Higher values of BSR led to uncontrolled agglomeration that can produce paste-like material which is unsuitable for downstream processing. On the other hand, the initial primary particle size and agitation rate parameters had a significant impact on the wetting, nucleation and layering timescales which affected the time to completion. However, the impact on the final equilibrium agglomerate attributes such as the agglomerate size and size distribution were small.

To improve further mechanistic understanding and enable spherical agglomeration as a key particle engineering technique for pharmaceutical manufacturing, validation of the kinetic parameters within the population balance model is essential. The power of the models is dependent on the quality of the model parameters and therefore, the ability to measure these parameters through off line characterisation experiments will be very helpful. Equally, sensitivity analysis of the model under various material systems and different regimes i.e., immersion nucleation would be beneficial.

6. References

[1] K. Plumb, Continuous processing in the pharmaceutical industry: changing the mind set, Chemical Engineering Research and Design, 83 (2005) 730-738.

[2] M.M. Nasr, M. Krumme, Y. Matsuda, B.L. Trout, C. Badman, S. Mascia, C.L. Cooney, K.D. Jensen, A. Florence, C. Johnston, Regulatory perspectives on continuous pharmaceutical manufacturing: moving from theory to practice: September 26-27, 2016, international symposium on the continuous manufacturing of pharmaceuticals, Journal of pharmaceutical sciences, 106 (2017) 3199-3206.

[3] C.J. Brown, T. McGlone, S. Yerdelen, V. Srirambhatla, F. Mabbott, R. Gurung, M.L. Briuglia, B. Ahmed, H. Polyzois, J. McGinty, F. Perciballi, D. Fysikopoulos, P. MacFhionnghaile, H. Siddique, V. Raval, T.S. Harrington , A.D. Vassileiou, M. Robertson, E. Prasad, A. Johnston, B. Johnston, A. Nordon, J.S. Srai, G. Halbert, J.H. ter Horst, C.J. Price, C.D. Rielly, J. Sefcik, A.J. Florence, Enabling precision manufacturing of active pharmaceutical ingredients: workflow for seeded cooling continuous crystallisations, Molecular Systems Design & Engineering, 3 (2018) 518-549.

[4] L. Rogers, N. Briggs, R. Achermann, A. Adamo, M. Azad, D. Brancazio, G. Capellades, G. Hammersmith, T. Hart, J. Imbrogno, Continuous production of five active pharmaceutical ingredients in flexible plug-and-play modules: a demonstration campaign, Organic Process Research & Development, 24 (2020) 2183-2196.

[5] Z.K. Nagy, A. El Hagrasy, J. Litster, Continuous pharmaceutical processing, Springer2020.

[6] L. Schenck, A. Koynov, A. Cote, Particle engineering at the drug substance, drug product interface: a comprehensive platform approach to enabling continuous drug substance to drug product processing with differentiated material properties, Drug Development and Industrial Pharmacy, 45 (2019) 521-531.

[7] A. Sirianni, C. Capes, J. Puddington, Recent experience with the spherical agglomeration process, The Canadian Journal of Chemical Engineering, 47 (1969) 166-170.

[8] J. Sutherland, The agglomeration of aqueous suspensions of graphite, The Canadian Journal of Chemical Engineering, 40 (1962) 268-272.

[9] Y. Kawashima, C. Capes, Further studies of the kinetics of spherical agglomeration in a stirred vessel, Powder Technology, 13 (1976) 279-288.

[10] Y. Kawashima, M. Imai, H. Takeuchi, H. Yamamoto, K. Kamiya, T. Hino, Improved flowability and compactibility of spherically agglomerated crystals of ascorbic acid for direct tableting designed by spherical crystallization process, Powder technology, 130 (2003) 283-289.
[11] K. Kedia, S. Wairkar, Improved micromeritics, packing properties and compressibility of high dose drug, Cycloserine, by spherical crystallization, Powder Technology, 344 (2019) 665-672.
[12] P.M. Orlewski, B. Ahn, M. Mazzotti, Tuning the particle sizes in spherical agglomeration, Crystal Growth & Design, 18 (2018) 6257-6265.
[13] A. Nokhodchi, M. Maghsoodi, D. Hassan-Zadeh, M. Barzegar-Jalali, Preparation of agglomerated crystals for improving flowability and compactibility of poorly flowable and compactible drugs and excipients, Powder technology, 175 (2007) 73-81.
[14] K. Pitt, R. Peña, J.D. Tew, K. Pal, R. Smith, Z.K. Nagy, J.D. Litster, Particle design via spherical agglomeration: A critical review of controlling parameters, rate processes and modelling, Powder Technology, 326 (2018) 327-343.
[15] S.M. Iveson, J.D. Litster, K. Hapgood, B.J. Ennis, Nucleation, growth and breakage phenomena in agitated wet granulation processes: a review, Powder technology, 117 (2001) 3-39.
[16] J. Litster, Scaleup of wet granulation processes: science not art, Powder Technology, 130 (2003) 35-40.
[17] C. Subero-Couroyer, D. Mangin, A. Rivoire, A. Blandin, J. Klein, Agglomeration in suspension of salicylic acid fine particles: Analysis of the wetting period and effect of the binder injection mode on the final agglomerate size, Powder technology, 161 (2006) 98-109.
[18] R. Peña, D.J. Jarmer, C.L. Burcham, Z.K. Nagy, Further understanding of agglomeration mechanisms in spherical crystallization systems: benzoic acid case study, Crystal Growth & Design, 19 (2019) 1668-1679.
[19] A.F. Blandin, A. Rivoire, D. Mangin, J.P. Klein, J.M. Bossoutrot, Using in situ image analysis to study the kinetics of agglomeration in suspension, Particle & Particle Systems Characterization: Measurement and Description of Particle Properties and Behavior in Powders and Other Disperse Systems, 17 (2000) 16-20.
[20] A. Blandin, D. Mangin, A. Rivoire, J. Klein, J. Bossoutrot, Agglomeration in suspension of salicylic acid fine particles: influence of some process parameters on kinetics and agglomerate final size, Powder technology, 130 (2003) 316-323.

[21] O. Arjmandi-Tash, J.D. Tew, K. Pitt, R. Smith, J.D. Litster, A new mathematical model for nucleation of spherical agglomerates by the immersion mechanism, Chemical Engineering Science: X, 4 (2019) 100048.
[22] R. David, A.-M. Paulaime, F. Espitalier, L. Rouleau, Modelling of multiple-mechanism agglomeration in a crystallization process, Powder Technology, 130 (2003) 338-344.
[23] D.R. Ochsenbein, T. Vetter, M. Morari, M. Mazzotti, Agglomeration of needle-like crystals in suspension. II. Modeling, Crystal Growth & Design, 15 (2015) 4296-4310.
[24] L. Madec, L. Falk, E. Plasari, Modelling of the agglomeration in suspension process with multidimensional kernels, Powder Technology, 130 (2003) 147-153.
[25] A.F. Blandin, D. Mangin, C. Subero-Couroyer, A. Rivoire, J.P. Klein, J.M. Bossoutrot, Modelling of agglomeration in suspension: Application to salicylic acid microparticles, Powder Technology, 156 (2005) 19-33.
[26] R. Peña, C.L. Burcham, D.J. Jarmer, D. Ramkrishna, Z.K. Nagy, Modeling and optimization of spherical agglomeration in suspension through a coupled population balance model, Chemical Engineering Science, 167 (2017) 66-77.
[27] D. Barrasso, R. Ramachandran, Qualitative assessment of a multi-scale, compartmental PBM-DEM model of a continuous twin-screw wet granulation process, Journal of Pharmaceutical Innovation, 11 (2016) 231-249.
[28] F. Perciballi, Formation of optimised particles for formulation and processing, University of Strathclyde, 2018.

7. Acknowledgements

This research was supported by EPSRC Future Continuous Manufacturing and Advanced Crystallisation Research Hub (CMAC, grant ref: EP/P006965/1). The authors are grateful to Dr F. Perciballi, Dr N. Rajoub, Dr C. Brown, Dr I. Houson and Prof A. Florence from the University of Strathclyde for sharing insightful experimental data on the spherical agglomeration process. The authors would also like to thank Dr N. Mitchell and Dr S. Bellinghausen from Siemens Process Systems Enterprise Ltd. (Siemens, PSE) for the implementation of customized models into the process-level population balance model in gPROMS FormulatedProducts.

8. CRediT Authorship Contribution Statement

Bilal Ahmed: Writing – original draft, Methodology, Software, Data curation.
Omid Arjmandi-Tash: Writing – original draft, Methodology, Software, Formal analysis.
James D. Litster: Conceptualization, Supervision, Writing – review & editing, Funding acquisition.
Rachel M. Smith: Conceptualization, Supervision, Writing – review & editing, Funding acquisition.

Appendix:

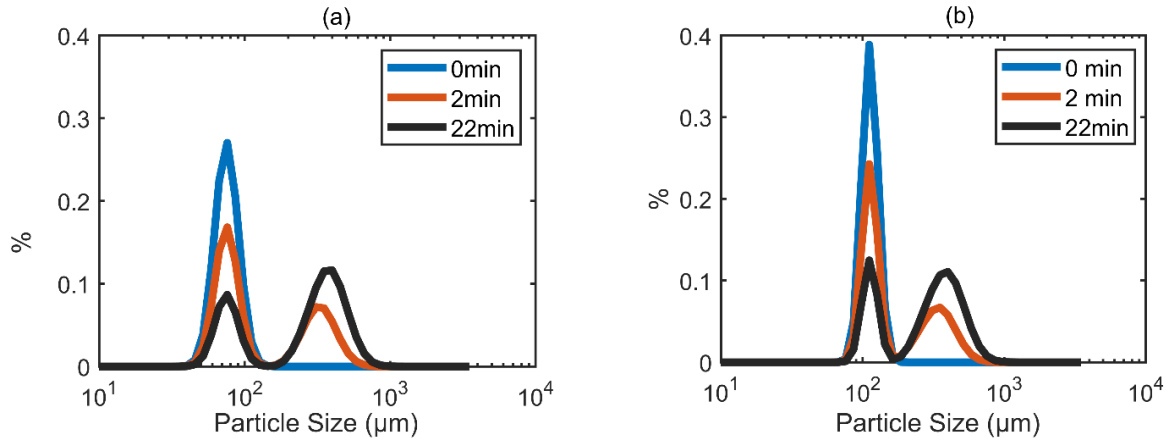

Figure A 1. Sensitivity of time evolution of agglomerate size for the initial mean primary particle sizes, D_p of (a) 80 μm and (b) 120 μm.

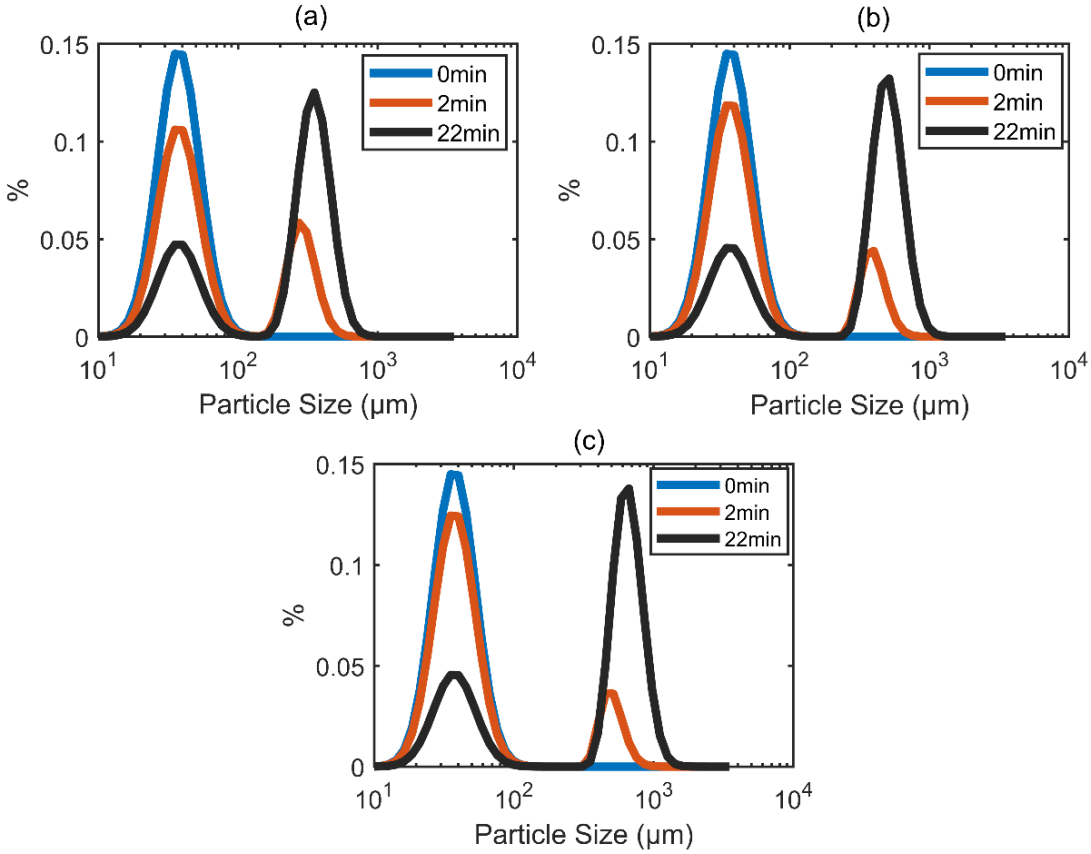

Figure A 2. Sensitivity of time evolution of agglomerate size for the mean bridging liquid droplet size, D_d (μm) of (a) 200 μm (b) 300 μm and (c) 400 μm.

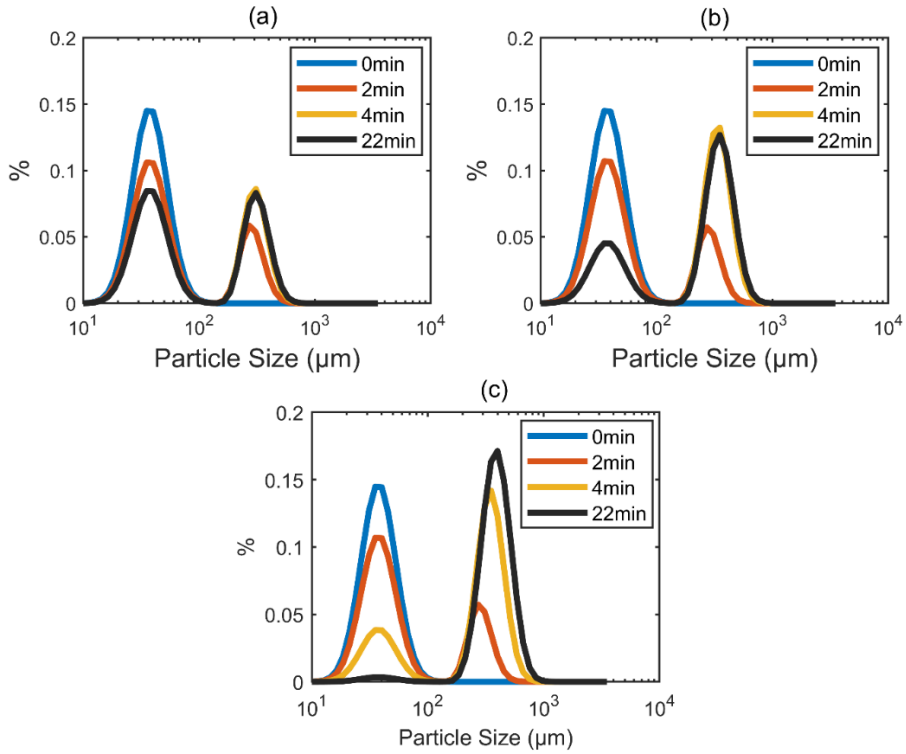

754

755 **Figure A 3.** Sensitivity of time evolution of agglomerate size for the bridging liquid to
756 solids ratio (BSR) of (a) 0.35 (b) 0.55 and (c) 0.75.

757

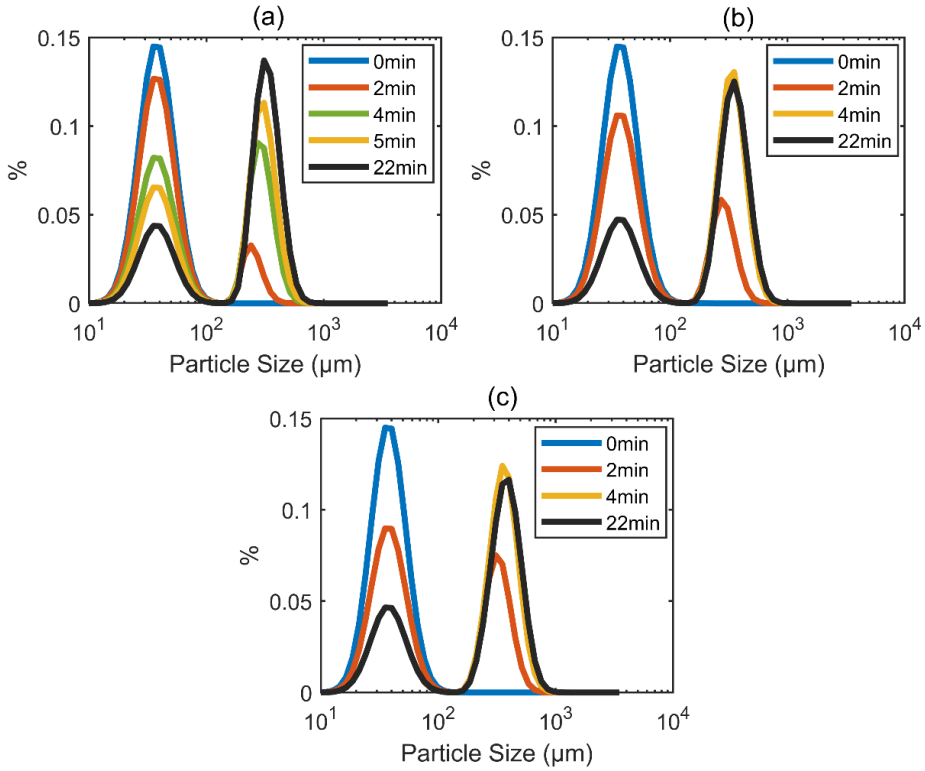

758

759 **Figure A 4.** Sensitivity of time evolution of agglomerate size for the agitation rate
760 (RPM) of (a) 200 (b) 300 and (c) 400.